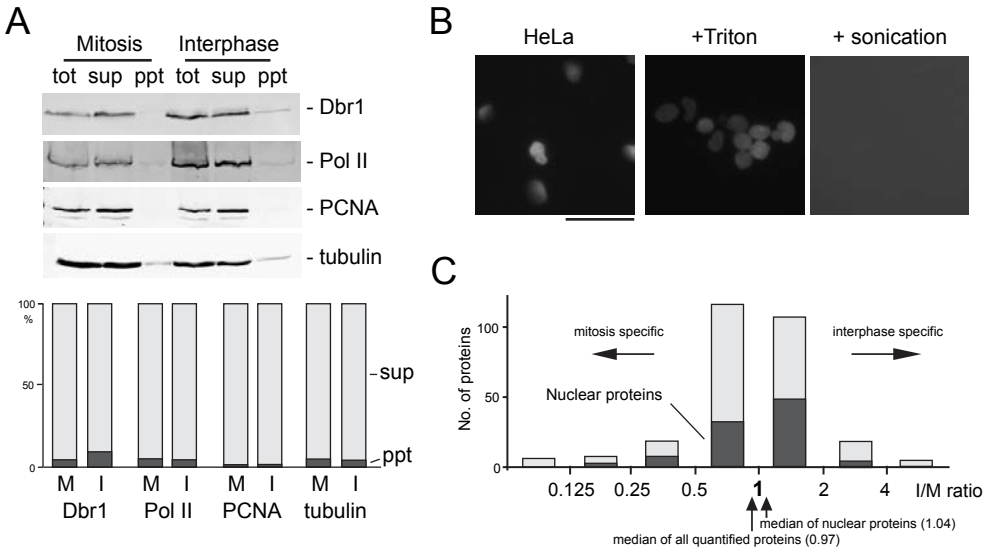
A
Mitosis
Interphase
tot sup ppt tot sup ppt
- Dbr1
- Pol II
- PCNA
- tubulin
100 %
50
0
sup
ppt
M I M I M I M I
Dbr1 Pol II PCNA tubulin
B
HeLa
+Triton
+ sonication
C
No. of proteins
100
50
0
mitosis specific
interphase specific
Nuclear proteins
0.125 0.25 0.5 1 2 4 I/M ratio
median of nuclear proteins (1.04)
median of all quantified proteins (0.97)

Figure S1

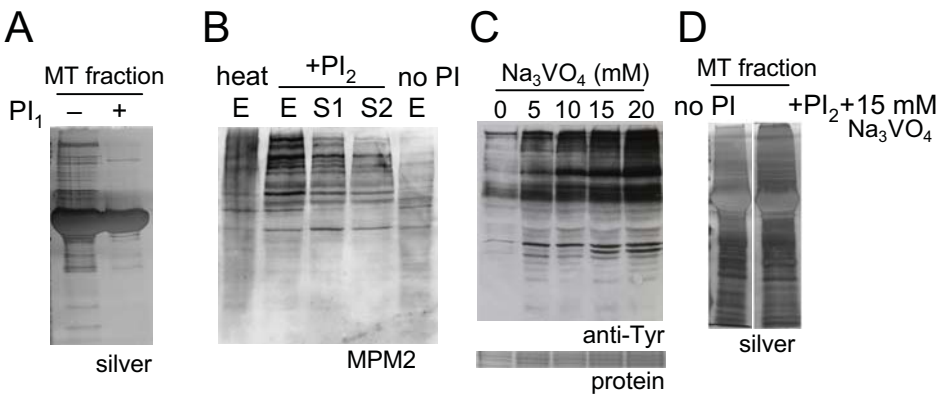
A
MT fraction
PI1 – +
silver
B
heat +PI2 no PI
E E S1 S2 E
MPM2
C
Na3VO4 (mM)
0 5 10 15 20
anti-Tyr
protein
D
MT fraction
no PI +PI2+15 mM Na3VO4
silver

Figure S2

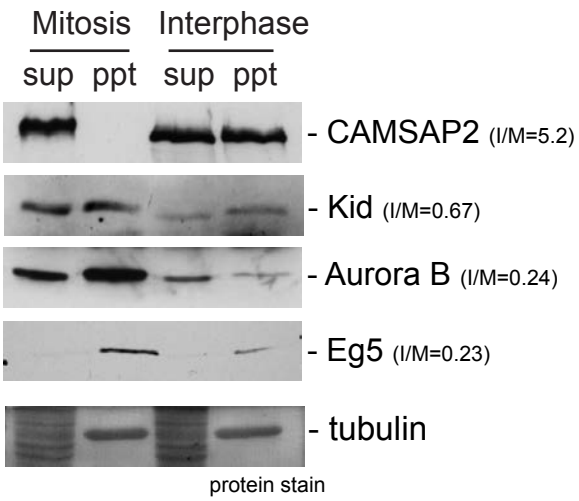
Mitosis
Interphase
sup
ppt
sup
ppt
- CAMSAP2 (I/M=5.2)
- Kid (I/M=0.67)
- Aurora B (I/M=0.24)
- Eg5 (I/M=0.23)
- tubulin
protein stain

Figure S3

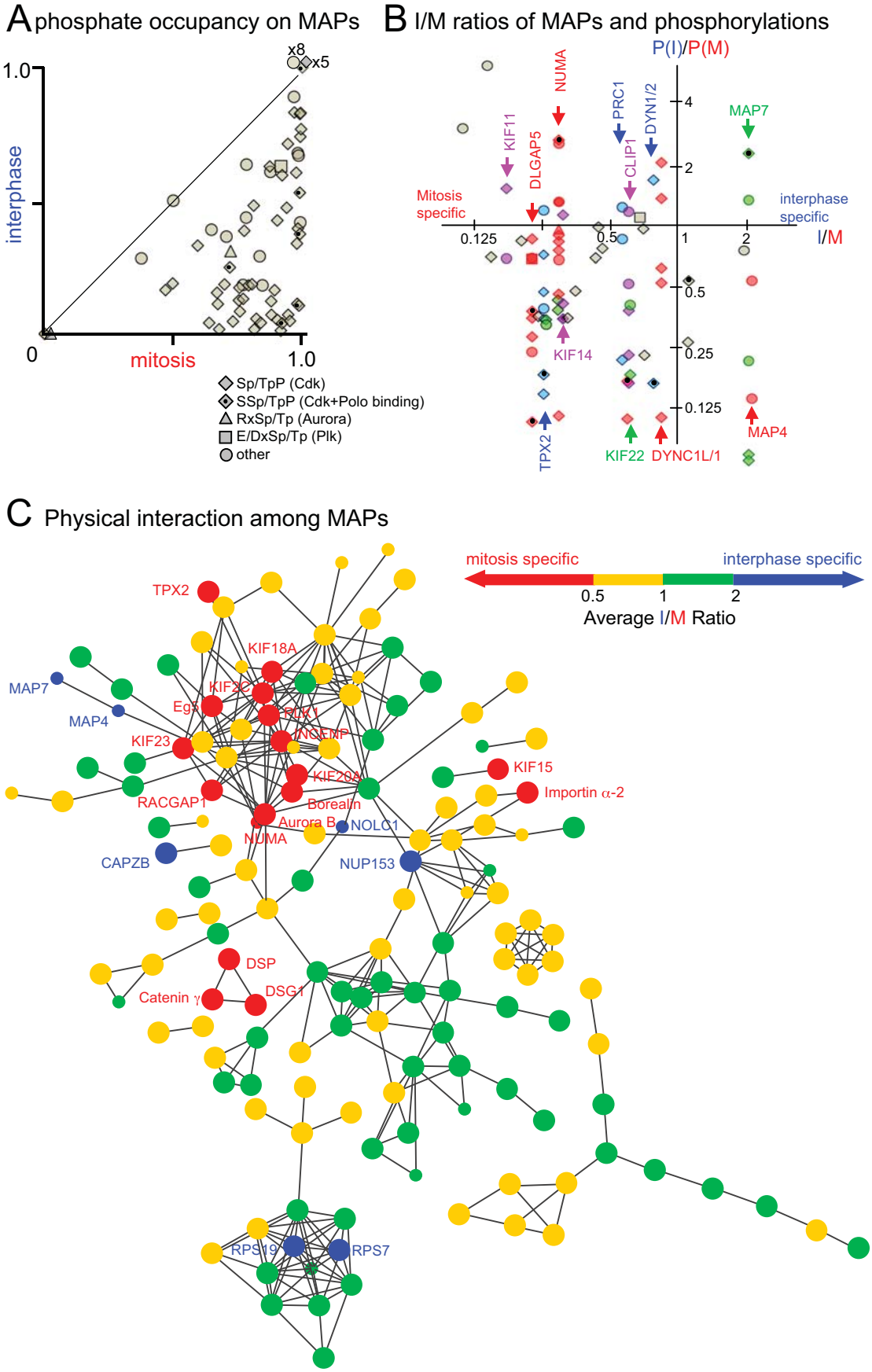
A phosphate occupancy on MAPs
x8
x5
1.0
interphase
0
mitosis
1.0
Sp/TpP (Cdk)
SSp/TpP (Cdk+Polo binding)
RxSp/Tp (Aurora)
E/DxSp/Tp (Plk)
other
B I/M ratios of MAPs and phosphorylations
P(I)/P(M)
NUMA
KIF11
DLGAP5
PRC1
CLIP1
DYN1/2
MAP7
Mitosis specific
interphase specific
0.125
0.5
1
2
I/M
4
2
0.5
0.25
0.125
KIF14
TPX2
KIF22
DYNC1L/1
MAP4
C Physical interaction among MAPs
mitosis specific
interphase specific
0.5
1
2
Average I/M Ratio
TPX2
KIF18A
MAP7
KIF2C
Eg5
PRC1
MAP4
INCENP
KIF23
KIF15
KIF20A
Importin α-2
RACGAP1
Borealin
Aurora B
NOLC1
NUMA
CAPZB
NUP153
DSP
Catenin γ
DSG1
RPS19
RPS7

Figure S4

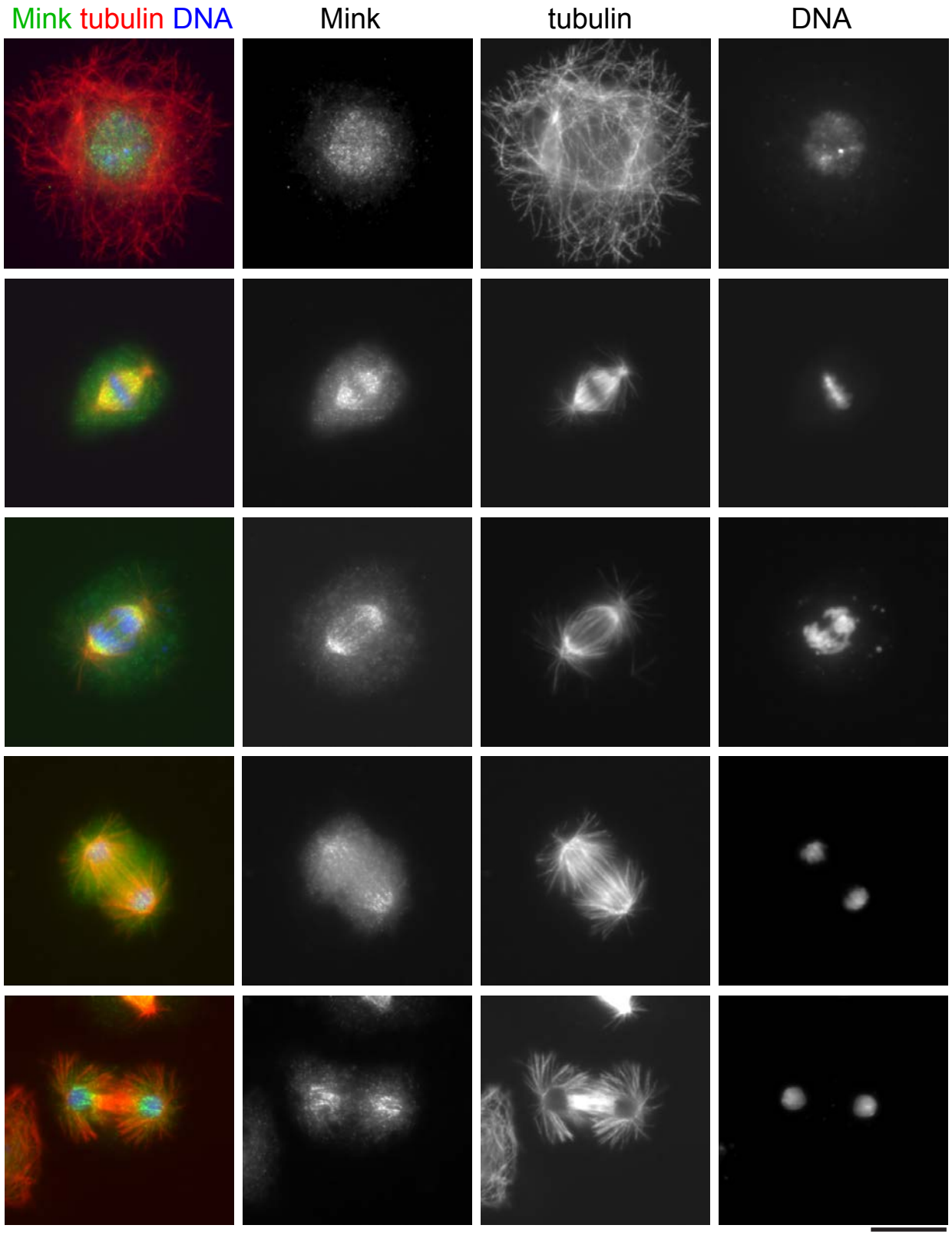

Figure S5

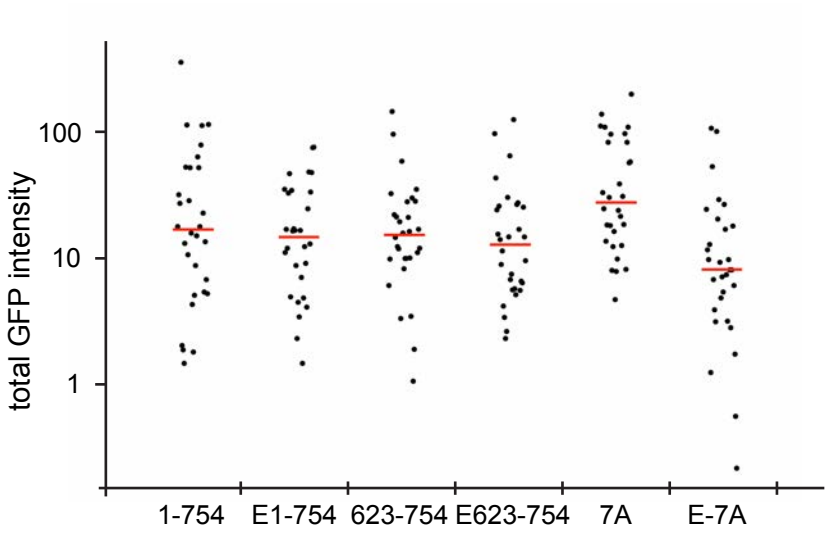
total GFP intensity
100
10
1
1-754
E1-754
623-754
E623-754
7A
E-7A

Figure S6

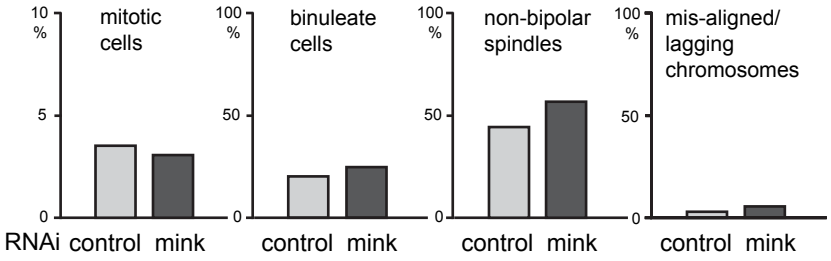
10
%
5
0
mitotic
cells
100
%
50
0
binuleate
cells
100
%
50
0
non-bipolar
spindles
100
%
50
0
mis-aligned/
lagging
chromosomes
RNAi control mink
control mink
control mink
control mink

Figure S7

Figure S1. Nuclear proteins were not removed during extract preparation. (A) Immunoblot of the total extract (tot), and supernatant (sup) and pellet (ppt) after the ultracetrifugation of mitotic (M) and interphase (I) extracts, using antibodies against α-tubulin and nuclear proteins (Dbr1, Pol II and PCNA). The bar graph indicates relative amounts of each protein found in the supernatant (light gray) and pellet (solid). (B) DAPI staining of intact HeLa cells, cell extracts after the addition of Triton-X100 or after sonication. Sonication, which is included in our routine sample preparation, completely disrupted nuclei. Bar=50 μm. (C) The number of all proteins and proteins assigned as "nuclear" (in Uniprot; solid bars) that are quantified in our SILAC experiments in each I/M ratio range.

Figure S2. Optimisation of phosphatase inhibitors to maintain protein phosphorylation in S2 cells
(A) Proteins co-sedimented with Taxol stabilised microtubules in the presence and absence of the phosphatase inhibitor mixture 1 (PI_1; 100 mM NaF, 15 mM p-nitrophenyl phosphate, 100 mM β-glycerophosphate and 2 μM okadaic acid). This phosphatase inhibitor mixture inhibits the protein binding to microtubules. (B) Phosphorylation of serine/threonine is maintained by phosphatase inhibior mixture 2 (PI_2; 10 mM p-nitrophenyl phosphate and 1 μM okadaic acid). A western blot was probed with MPM2 antibody which recognises a subset of serine/threonine phosphorylation. Heat E; crude extract from cells lysed in hot sample buffer to instantly inactivate endogenous phosphatases. E; soluble extract prepared in buffer containing PI_2. S1; the supernatant after microtubule co-sedimentation. S2; the supernatant after spinning down without microtubule polymerisation. no PI E; soluble extract prepared in buffer without phosphatase inhibitors. (C) Na_3VO_4 maintained phosphorylation of tyrosine. Soluble extract was prepared in buffer containing the phosphatase inhibior mixture 2 and different concentrations of Na_3VO_4, and tested by a western blot probed with an anti-tyrosine antibody. (D) Proteins co-sedimented with Taxol-stabilised microtubules in the presence and absence of the phosphatase inhibitor mixture 2 and 15 mM Na_3VO_4.

Figure S3. Immunoblots confirm SILAC results. Immunoblots of the supernatant (sup) and pellet (ppt) after microtubule co-sedimentation using antibodies against proteins with various I/M ratios. The bottom panel shows the total protein staining.

Figure S4. Phosphorylation and interactions among MAPs.
(A) The estimated absolute phosphate occupancy at each site in MAP fraction in mitosis (the X-axis) and interphase (the Y-axis). The shape of each dot represents a match to a kinase consensus sequence. This includes only phosphorylation sites that have both the I/M ratios of a phosphopeptide and the corresponding non-phosphopeptide, as they are essential for estimation of absolute occupancies. (B) A change of phosphorylation in the MAP fraction between mitosis and interphase in HeLa cells. The X-axis shows the I/M ratio of protein in the MAP fractions, while the Y-axis shows the relative phosphate occupancies at each site found in MAP fractions in interphase in comparison to in mitosis. This graph includes all phosphorylation sites quantified from the second experiment. The shape of each dot represents a match to a kinase consensus sequence. Vertically aligned dots with the same colour indicates multiple phosphorylations found on the same protein. Grey dots indicate single protein phosphorylations. (C) Interaction map among MAPs. Lines, circles and the fill colours of circles represent known physical interactions, MAPs and their average I/M ratios. The protein names are shown for MAPs with average I/M ratios outside of 0.5-2. STRING was used to identify known interactions and create the map.

Figure S5. Mink localisation during the cell cycle. Immunostaining of S2 cells using antibodies against Mink and α-tubulin, and counterstained with DAPI. Bar=10 μm.

Figure S6. Expression of GFP-tagged Mink and variants in transfected cells. The total fluorescent intensity of GFP within each transfected cell is plotted. The median value is indicated by the horizontal bar. The microtubule binding domain alone (623-754, E623-754) and non-phosphorylatable forms (7A, E-7A) that show defects at a high frequency were not expressed more than a full-length Mink (1-754, E1-754).

Figure S7. The cytological phenotype after the depletion of Mink protein. S2 cells were incubated with double stranded RNA corresponding to *mink* and control (β-lactamase gene). The frequencies of mitotic cells (phospho-H3 Ser10 positive), and binucleate interphase cells are relative to all cells. The frequencies of non-bipolar spindles and mis-aligned/lagging chromosomes are relative to mitotic cells. No significant differences were observed between control and *mink* RNAi.